

# Color Constancy using Achromatic Surface

Bing Li,<sup>1\*</sup> De Xu,<sup>1</sup> Weihua Xiong,<sup>2</sup> Songhe Feng<sup>1</sup>

<sup>1</sup>Institute of Computer Science and Engineering, Beijing Jiaotong University, Beijing 100044, China

<sup>2</sup>OmniVision Technologies, Sunnyvale, CA 95014

Received 23 June 2008; revised 18 March 2009; accepted 20 April 2009

*Abstract:* Although a number of elaborate color constancy algorithms have been proposed, methods such as Grey World and Max-RGB are still widely used because of their low computational costs. The Grey World algorithm is based on the grey world assumption: the average reflectance in a scene is achromatic. But this assumption cannot be always satisfied well. Borrowing on some of the strengths and simplicity of the Grey World algorithm, W. Xiong et al. proposed an advanced illumination estimation method, named Grey Surface Identification (GSI), which identifies those grey surfaces no matter what the light color is and averages them in RGB space. However, this method is camera-dependent, so it cannot be applied on the images from unknown imaging device. Motivated by the paradigm of the GSI, we present a novel iteration method to identify achromatic surface for illumination estimation. Furthermore, the local Grey Edge method is introduced to optimize the initial condition of the iteration so as to improve the accuracy of the proposed algorithm. The experiment results on different image datasets show that our algorithm is effective and outperforms some current state-of-the-art color constancy algorithms. © 2010 Wiley Periodicals, Inc. Col Res Appl, 00, 000–000, 2010; Published online in Wiley InterScience (www.interscience.wiley.com). DOI 10.1002/col.20574

*Key words:* color constancy; illumination estimation; achromatic surface identification

\*Correspondence to: Bing Li (e-mail: bjtulb@gmail.com).

Contract grant sponsor: National Nature Science Foundation of China; contract grant numbers: 60803072, 90820013.

Contract grant sponsor: National High Technology Research and Development Program of China; contract grant number: 2007AA01Z168.

Contract grant sponsor: Science Foundation of Beijing Jiaotong University; contract grant number: 2007XM008.

## INTRODUCTION

As a simple and straightforward clue, color has been used in many computer vision applications, such as object recognition and tracking, scene understanding, image reproduction, as well as photography. However, the color information of any image recorded by a camera depends on three factors: the physical content of the scene, the illumination incident on the scene, and the characteristics of the camera.<sup>1,2</sup> Different light sources will result in different colors of the same object surface. Color constancy refers to the genre of techniques that aim to recognize the color of objects invariant of the color of the light source. It generally includes two steps<sup>3</sup>: Firstly, estimate the color of light source from image data. Secondly, the von Kries diagonal transformation is applied on the image to get the objects' color under a known canonical light source.<sup>4</sup>

Past decades have witnessed significant progress in color constancy algorithms. All these solutions can be roughly divided into two major categories: unsupervised approaches and supervised ones. The algorithms falling in the first category are straightforward as they are based on the nature of the color components of image itself. Max-RGB estimates the light source color from the maximum response of the different color channels.<sup>2</sup> It assumes that the brightest point in the scene is white, meaning that the red, green, and blue values of the point represent the illumination features. Another well-known algorithm is Grey World algorithm, which assumes that the average reflectance in the scene is achromatic.<sup>5</sup> By using Minkowski-norm, G.D. Finlayson *et al.*<sup>6</sup> proposed Shades of Grey (SoG) algorithm, which can integrate Max-RGB and Grey World algorithms into a uniform framework. More recently, Weijier *et al.*<sup>3,7</sup> presented another Grey Edge hypothesis: The average of the reflectance differences in a scene is achromatic. Based on this hypothesis, edge-based color constancy algorithm, which uses high-order derivative image to estimate illumination, was given out. Xiong<sup>8</sup>

proposed a novel illumination color estimation solution, called Grey Surface Identification (GSI), by detecting those potential grey surfaces in the scene through a specific coordinate system and averaging them in the RGB space. The other color constancy category includes those training-based solutions, the ingredients that they have in common is to build up the relationship between image color distribution and light attribute. The first important method is Bayesian color constancy introduced by Brainard and Freeman.<sup>9</sup> It requires having a prior knowledge about the reflectance in real scenes and the distribution of light sources. However, it is very computationally expensive because the number of parameters is a function of the number of surfaces. Another problem of this method is that it depends on the performance of image segmentation. A more practical solution is color by correlation proposed by Finlayson.<sup>10</sup> In essence, this algorithm is a discrete implementation of Bayesian concept. It establishes a correlation matrix that describes the interrelation between illuminants and image chromaticity distribution. The best estimate of the specific illuminate incident on the image is chosen, having the highest probability among all potential ones. Barnard *et al.*<sup>11</sup> improved the promising method by extending it into 3D color space. Besides the chromaticity, the extra information used is pixel brightness. The common limitation of these two methods is the requirement of having various predefined illuminations as the prediction is chosen from one of them. This limitation can be elegantly addressed with Neural Network, which inherently includes a model of joint probability.<sup>12</sup> The neural network is fed with a binary chromaticity histogram and its output can be any arbitrary illumination values. Recently, better results have been achieved by using support vector regression that minimizes the structure risk without knowing the expected distribution of the image data.<sup>13,14</sup> Interpolation was also recently proved to be an efficient technique.<sup>15</sup> In this method, the illumination estimation is treated as a problem of interpolating over a set of uniformly sampled thumbnails created by averaging adjacent pixels in the original images. Other interesting solutions include color constancy by KL-divergence<sup>16</sup> and illumination color by voting.<sup>17</sup>

A complete review and comparison of color constancy algorithms can be found in.<sup>1,2,18</sup> Although statistical-based methods have been shown to be superior to the others, image-based color constancy solutions, such as Grey World, Max-RGB, SoG, and GSI, are still widely used in practical applications due to low computational cost and simplicity.<sup>3,19</sup> The Grey World algorithm has even been extended to color constancy for multiple illuminants.<sup>18,20</sup> In particular, GSI is drawing more attention as it can bring more accurate performance without adding more complexity. However, the potential grey pixel detection of this method is camera dependent and suffers from calibration requirement. In this article, we propose an iterative camera independent achromatic surface identification method and use R/G/B values of these surfaces to estimate the illumination's color information. We name the method Color Constancy using Achromatic Surface (CCAS).

The remainder of this article is organized as follows. In Section 2, after reviewing Grey World, SoG, and GSI algorithms, we explain the details of CCAS. The experimental results on different image datasets are presented next. Then finally the Conclusion.

## COLOR CONSTANCY USING ACHROMATIC SURFACE

### Grey World, Shades of Grey, and Grey Surface Identification Algorithms Review

According to the Lambertian reflectance model, the image  $f = (R, G, B)^T$  can be computed as follows:

$$f(X) = \int_{\omega} e(\lambda)S(X, \lambda)c(\lambda)d\lambda \quad (1)$$

where  $X$  is the spatial coordinate,  $\lambda$  is wavelength, and  $\omega$  represents the visible spectrum.  $e(\lambda)$  is spectrum of light source, the surface reflectance is denoted as  $S(X, \lambda)$ , and the camera sensitivity function is given by  $c(\lambda) = (R(\lambda), G(\lambda), B(\lambda))^T$ . The goal of color constancy is to estimate  $e$ :

$$e = \int_{\omega} e(\lambda)c(\lambda)d\lambda \quad (2)$$

Because both  $e(\lambda)$  and  $S(X, \lambda)$  are unknown, it is an underconstrained problem and it cannot be solved without any further assumptions. The Grey World algorithm is based on the grey world assumption, i.e., the average reflectance in a scene is achromatic. The assumption can be described as follows:

$$\frac{\int S(X, \lambda)dX}{\int dX} = k \quad (3)$$

where  $k$  is a constant, representing the chromaticity. Then, the light source color can be estimated by computing the average pixel value:

$$\begin{aligned} \frac{\int f(X)dX}{\int dX} &= \frac{\int_{\omega} \int e(\lambda)S(\lambda, X)c(\lambda)d\lambda dX}{\int dX} \\ &= k \int_{\omega} Le(\lambda)c(\lambda)d\lambda = ke \quad (4) \end{aligned}$$

Finlayson *et al.*<sup>6</sup> proposed a more general color constancy algorithm based on the Minkowski-norm and called it Shades of Grey (SoG). This algorithm is computed as:

$$\left( \frac{\int (f(X))^p dX}{\int dX} \right)^{1/p} = ke \quad (5)$$

For  $p = 1$ , the equation reduces to Grey World algorithm. For  $p = \infty$ , it is equal to Max-RGB algorithm. They also found that the best performance result can be obtained when  $p$  is set to be 6. Consequently, we will also apply SoG ( $p = 6$ ) on the R/G/B values of identified achromatic pixels to predict the illumination color.

Grey World and SoG use all pixels in the image to estimate light chromaticity values. A more reasonable trick is to identify those grey surfaces and use them to solve color constancy problem. Under some assumption and constraints, Finalyson *et al.* proved that varying the illumination's color temperature or its intensity of a surface will cause  $(\log R, \log G, \log B)$  to move within a plane and the planes from different surface reflectance are parallel to each other.<sup>21</sup> Based on this conclusion, Xiong *et al.* further proposed a new coordinate system, named LIS, that represents illumination ('L'), reflectance ('S'), and intensity ('I') as separately as possible.<sup>8,19</sup> The potential grey surfaces, no matter what the lighting condition is, can be gained if they have an S axis of nearly zero and only these pixels' R/G/B values are averaged to get the light color.

## Achromatic Surface Identification using Iteration

From previous section, we can see that the key point of GSI is to detect those potential grey pixels through a transformation between R/G/B space and LSI coordinate system. But this transformation requires calibrating the imaging device.<sup>8,19</sup> Therefore, it will inevitably fail on those images from any unknown cameras. Inspired by the basic idea of GSI, we develop an iterative achromatic surface identification method from the image itself. The SoG method is applied on the R/G/B values of these detected surfaces, and its output will be served as illumination color.

Before describing the CCAS algorithm, we define some functions and variants that will be used. The function  $isAch(px)$  is used to decide whether the pixel is potentially achromatic or not, it is defined as:

$$isAch(px) = \begin{cases} 1 & \text{if } \left| \frac{R}{B} - 1 \right| < \tau \text{ and } \left| \frac{G}{B} - 1 \right| < \tau \text{ and } (R \neq 0, G \neq 0, B \neq 0) \\ 0 & \text{else} \end{cases} \quad (6)$$

where  $px$  represents the pixel,  $R, G, B$  are the values of each color channel of pixel  $px$  in the image  $F'$ , which is the adjusted image under canonical illumination by estimated illumination color. Threshold  $\tau$  indicates the closeness among R/G/B values and it is empirically set to be 0.1 in this article. Besides  $\tau$ , the angular error threshold  $\varepsilon$  and iteration times threshold  $CTimes$  are also used to control the algorithm performance and efficiency. To alleviate the effect of image noise, we also define another pixels number threshold  $Tnum$  to determine whether there exists enough achromatic surface in the scene. The brief steps of proposed algorithm are as follows:

Step 1. Set  $i = 0$ . Suppose all the pixels in the image  $F$  are achromatic. Therefore the achromatic pixel set  $I_i$ :  $I_i = F$ . Estimate the illumination color  $e_i$  by applying SoG algorithm on all pixels in set  $I_i$ .

Step 2. Use the diagonal model<sup>4</sup> to map the image  $F$  to  $F'$ , which is the image under canonical illumination according to the estimated illumination  $e_i$ .

Step 3. Set  $i = i + 1$ . Select out the achromatic pixels from image  $F'$  to compose the new achromatic set  $I_i$  as:  $I_i = \{px | isAch(px) = 1\}$ . Where the function  $isAch(px)$  is defined in Eq. (6).

Step 4. If  $Num(I_i) < Tnum$ , where  $Num(I_i)$  is the total pixel number in set  $I_i$ , then return  $e_i$ . otherwise, estimate the illumination color  $e_i$  by applying SoG algorithm on updated pixel set  $I_i$  and compute the angular error  $Terr = angular(e_{i-1}, e_i)$ , where the function  $()$  is angular error defined in Section 3 [Eq. (12)].

Step 5. If  $Terr > \varepsilon$  or  $i \geq CTimes$ , return  $e_i$  and stop the procedure;

Otherwise go back to Step 2.

In the above steps, if  $Num(I_i) > Tnum$ , we believe that the achromatic pixels in the image are not enough for illu-

mination estimation, the algorithm returns the previous result  $e_{i-1}$ . Therefore, if  $Num(I_i) > Tnum$ , the CCAS will reduce to the SoG algorithm.  $Tnum$  is always set to be 1000 in our experiments. Figure 1 shows an example of the achromatic surface detection results. The identified achromatic surfaces after first iteration are marked in 'White' in Fig. 1(B). Figure 1(C) is the final results after three iterations. It shows that nearly all the achromatic surfaces are picked out correctly.

## Optimization of the Initial Condition

The initial value used by the iterative algorithm is very crucial for the result we obtained. The simplest way is to assume that all the pixels in the image are achromatic. That is, the initial condition defined in Subsection 2.2 is from the output of global Grey World. In this subsection, to improve the accuracy, we use the local Grey Edge to optimize the initial condition of the proposed algorithm, which is called CCAS (optimized). In some color constancy algorithms, a local Grey World<sup>22,23</sup> is used as the illumination of the spatial position  $X$ , which can be described as:

$$e(X) = f^\sigma(X) = f(X) \otimes G^\sigma \quad (7)$$

where  $e(X)$  is the illumination color of the spatial position  $X$ .  $f^\sigma(X) = f(X) \otimes G^\sigma$  is the convolution of the image  $f(X)$  with a Gaussian filter with scale parameter  $\sigma$ . This local Grey World algorithm has an obvious problem; the estimated illumination color will bias to the pixel's color in the uniformed region. To avoid this situation, by introducing Grey Edge algorithm,<sup>3,8</sup> we use local Grey Edge instead of local Grey World for local illumination estimation, which can be represented as Eq. (8).

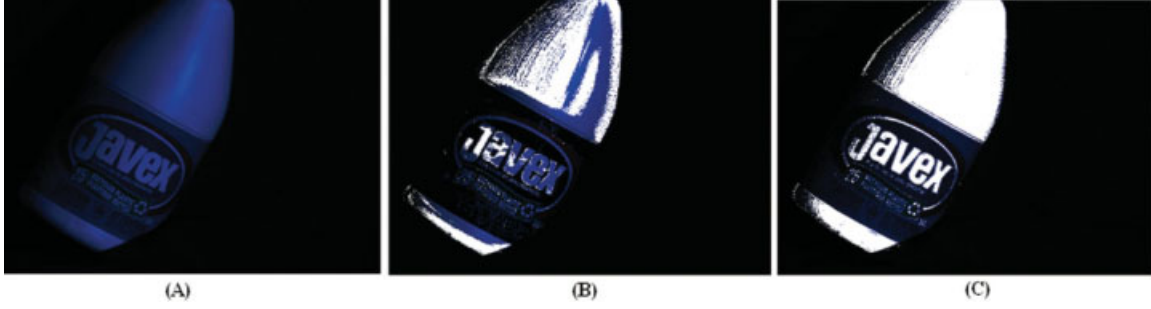


FIG. 1. An example of achromatic surface identification. The white color means these pixels are achromatic. (A) is original image. (B) is the identification result after first iteration, pixels identified as achromatic are indicated in white. (C) is the final result using CCAS, pixels identified as achromatic are indicated in white.

$$e(X) = f_X^\sigma(X) = (R_X^\sigma, G_X^\sigma, B_X^\sigma)^T \quad (8)$$

where the subscript  $X$  indicates the spatial derivative at scale  $\sigma$ . Assuming sensor sensitivity functions are narrow-band enough to follow the Dirac delta function,<sup>24</sup> according to Eq. (1) and Eq. (8), we obtain (9):

$$f(X) = S_c(X)E_c \Rightarrow S_c(X) = \frac{f(X)}{E_c} = \frac{f(X)}{f_X^\sigma(x)} \quad (9)$$

where  $S_c(X) = S(X, \lambda^c)$  and  $E_c = e(\lambda^c)$ .  $\lambda^c$  is the central wavelength for each channel. From Eq. (9), we can find

$$apAch(px) = \begin{cases} 1 & \text{if } \left| \frac{d_1}{d_2} - 1 \right| < \tau \text{ and } \left| \frac{d_2}{d_3} - 1 \right| < \tau \text{ and } d_k \neq 0 \quad (k = 1, 2, 3) \\ 0 & \text{else} \end{cases} \quad (10)$$

Now the initial condition (*Step 1*) in Section 2.2 can be optimized as:

Step 1. Set  $i = 0$ . Select out the achromatic pixels from image  $F$  to compose the original achromatic set  $I_i$  as:  $I_i = \{px | apAch(px) = 1\}$ . If  $Num(I_i) < Tnum$ ,  $I_i = F$ . Estimate the illumination color  $e_i$  by applying SoG algorithm on all pixels in set  $I_i$ .

Now, we can see that, if the total number of detected grey pixels from color invariant technique is too small, i.e.,  $Num(I_0) < Tnum$ , the algorithm CCAS(optimized) will reduce to the CCAS.

To check the effect of the optimized initial step and select the best  $\sigma$  for the descriptor  $D$ , we use the optimized initial step to estimate the initial illumination and compare its performance with SoG algorithm in the initial step of the original CCAS. The median angular error is used as the evaluating indicator. This comparison experiment is done on the 321 SFU Image Dataset. The detail of the 321 SFU Image Dataset and median angular error will be introduced in Sections 3.1 and 3.2. The experiment results are shown in Fig. 2.

From the experiment results, we can conclude that the optimization with local Grey Edge can significantly

that  $\frac{f(X)}{f_X^\sigma(X)}$  can approximately represent the object's surface reflectance. Consequently, we will construct a surface reflectance descriptor for the image edge region as  $D = \{d_1, d_2, d_3\} = \left\{ \frac{R}{R_X^\sigma}, \frac{G}{G_X^\sigma}, \frac{B}{B_X^\sigma} \right\}$  ( $R_X^\sigma \neq 0, G_X^\sigma \neq 0, B_X^\sigma \neq 0$ ).

By using descriptor  $D$ , we will get achromatic pixels from image edges with  $d_1 \approx d_2 \approx d_3$  ( $d_k \neq 0, k = 1, 2, 3$ ) to compose the initial achromatic pixel set instead of using all the pixels in CCAS. Here, we introduce a new function  $apAch(px)$  to extract those achromatic pixels from original input image, shown in Eq. (10).

improve the initial illumination estimation accuracy than Shade of Grey algorithm. The best value can be reached if we set  $\sigma = 4$ . The value will also be used in the following experiments.

Figure 3 gives another example, showing that the presented optimization solution can improve the performance of achromatic surface identification. Figure 3(A) is the original image. Figure 3(B) is the identification result after first iteration of CCAS(optimized). Figure 3(C) is the

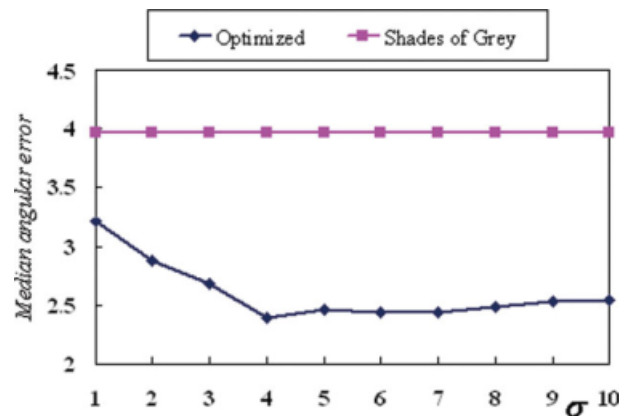


FIG. 2. The median angular error of the optimized initial step changes with the  $\sigma$ .





FIG. 3. An example of achromatic surface identification. The white color means these pixels are achromatic. (A) is original image. (B) is the identification result after first iteration of CCAS (optimized), pixels identified as achromatic are indicated in white. (C) is the final identification result using optimized initial condition. (D) is the final identification result iterations using original CCAS, pixels identified as achromatic are indicated in white.

final identification result using optimized initial condition. Figure 3(D) is the final identification result iterations using original CCAS. Some achromatic surfaces that are not identified using normal solution, shown in Fig. 3(D), which can now be detected out by using optimized initial condition, shown in Fig. 3(C).

### EXPERIMENTS

The two thresholds in the proposed algorithm, which is used to control iteration, are set as follows: The angular error threshold  $\varepsilon = 0.5$  and iteration times threshold  $CTimes = 5$ . We evaluate the proposed algorithm and compare it with others on three real image datasets. The first one is Barnard's set of 321 SFU images,<sup>25</sup> the second one is Cardei's 900 uncalibrated images from different cameras<sup>12</sup>; the last experiment are tested on Ciurea *et al.*<sup>26</sup> indoor and outdoor images captured from a digital video.

### Error Measure

Several error measures are used to evaluate performance of the proposed algorithms. For each image, the distance  $E_d$  between the measured actual illumination

chromaticity  $(r_a, g_a)$  and the estimated illumination  $(r_e, g_e)$  is calculated as:

$$E_d = \sqrt{(r_a - r_e)^2 + (g_a - g_e)^2} \quad (11)$$

Assuming there are  $N$  test images, we will also report root mean square (RMS), maximum and median distance.<sup>8,19,27</sup> The RMS of the chromaticity distance  $RMS_d$  is defined as:

$$RMS_d = \sqrt{\frac{1}{N} \sum_{i=1}^N E_d^2(i)} \quad (12)$$

where the  $E_d(i)$  is the illumination chromaticity distance error of  $i$ th image. The angular error  $E_a$  between the measured actual illumination chromaticity  $e_a = (r_a, g_a, b_a)$  and the estimated illumination  $e_e = (r_e, g_e, b_e)$  is also used. The angular error function  $angular(e_a, e_e)$  is defined as:

$$E_a = angular(e_a, e_e) = \cos^{-1} \left( \frac{(r_a, g_a, b_a)(r_e, g_e, b_e)}{\sqrt{r_a^2 + g_a^2 + b_a^2} \times \sqrt{r_e^2 + g_e^2 + b_e^2}} \right) \times \frac{180^\circ}{\pi} \quad (13)$$

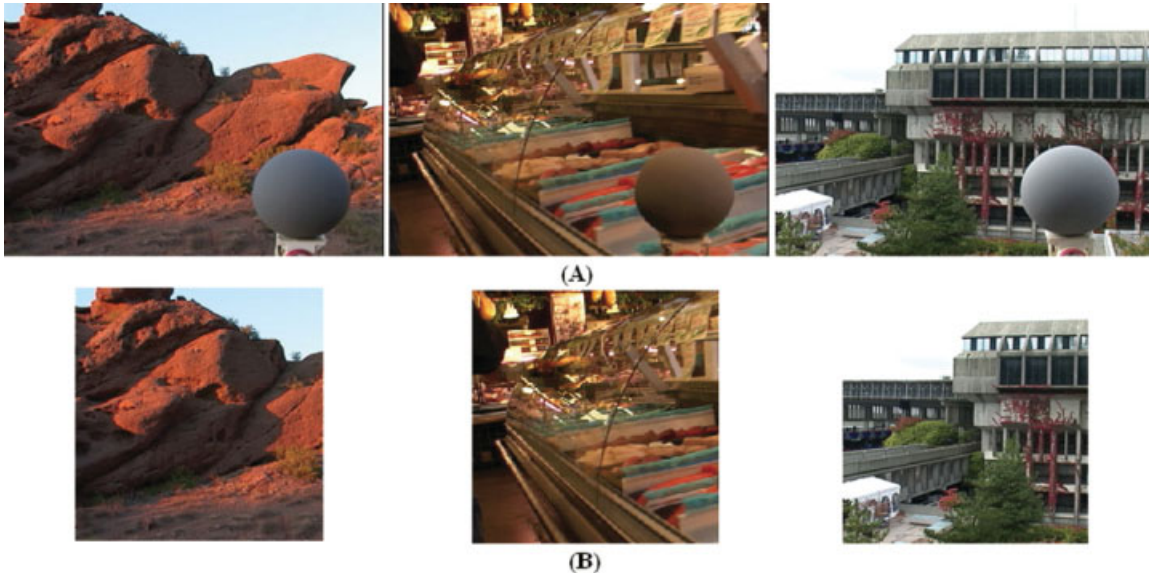


FIG. 4. (A) Examples of the images from the 11,346 real-world image set. (B) Cropped images for experiments.

TABLE I. Comparison of CCAS to Max\_RGB, Grey World, Shades of Grey, and Grey-Edge performance.

Method	Parameters	Median angle	Max angle	RMS angle	Median dist ( $\times 10^2$ )	Max dist ( $\times 10^2$ )	RMS dist ( $\times 10^2$ )
Max_RGB*	-	6.44	36.24	12.28	4.46	25.01	8.25
Grey World*	-	7.04	37.31	13.58	5.68	35.38	11.12
SoG*	$p = 6$	3.97	28.70	9.027	2.83	19.77	6.21
Grey-Edge	$e^{1,7,4}$	3.20	31.57	8.30	2.37	20.13	5.81
Second-order Grey-Edge	$e^{2,7,5}$	2.74	26.75	7.75	2.03	17.74	5.47
CCAS	$\varepsilon = 0.5, p = 6,$	2.49	29.66	8.28	1.83	19.65	5.49
CCAS (optimized)	$C_{Times} = 5,$ $T_{num} = 1000$	2.18	27.17	7.32	1.61	19.14	4.94

The tests are based on the 321 indoor images. The results of other algorithms marked by "\*" are from Ref 19.

TABLE II. Comparison of CCAS to other algorithms via the Wilcoxon signed-rank test.

	Max_RGB	Grey-World	SoG	Grey-Edge	Second-order Grey-Edge	CCAS	CCAS (optimized)
Max_RGB		-	-	-	-	-	-
Grey World	+		-	-	-	-	-
SoG	+	+		-	-	-	-
Grey-Edge	+	+	+		-	-	-
Second-order Grey-Edge	+	+	+	+		=	-
CCAS	+	+	+	+	=		-
CCAS (optimized)	+	+	+	+	+	+	

A '+' means the algorithm listed in the row is statistically better than the one in the column. A '-' indicates the opposite, and an '=' indicates that the performance difference of these two algorithms is statistically trivial.

TABLE III. Comparison of CCAS to Max\_RGB, Grey-World, Shades of Grey, and Grey-edge performance.

Method	Parameters	Median angle	Max angle	RMS angle	Median dist ( $\times 10^2$ )	Max dist ( $\times 10^2$ )	RMS dist ( $\times 10^2$ )
Max_RGB*	-	2.96	27.16	6.39	2.17	22.79	4.75
Grey World*	-	4.34	31.44	6.65	3.17	29.99	5.26
SoG*	$p = 6$	3.02	19.71	4.99	2.19	15.96	3.80
Grey-Edge	$e^{1,7,4}$	3.27	31.76	5.79	2.44	28.15	4.40
Second-order Grey-Edge	$e^{2,7,5}$	3.34	34.98	5.85	2.53	31.08	4.48
CCAS	$\varepsilon = 0.5, p = 6,$	2.26	19.60	4.72	1.63	14.90	3.59
CCAS (Optimized)	$C_{Times} = 5,$ $T_{num} = 1000$	2.07	19.43	4.32	1.51	13.85	3.24

The tests are based on the 900 uncalibrated images. The results of other algorithms marked by "\*" are from Ref. 19.

TABLE IV. Comparison of CCAS to other algorithms via the Wilcoxon signed-rank test.

	Max_RGB	Grey-World	SoG	Grey-Edge	Second-order Grey-Edge	CCAS	CCAS (Optimized)
Max_RGB		+	=	+	+	-	-
Grey World	-		-	-	-	-	-
SoG	=	+		+	+	-	-
Grey-Edge	-	+	-		=	-	-
Second-order Grey-Edge	-	+	-	=		-	-
CCAS	+	+	+	+	+		-
CCAS (Optimized)	+	+	+	+	+	+	

The labelings '+' '-' and '=' have same meanings as those shown in Table II.

TABLE V. Comparison of CCAS to Max\_RGB, Grey-World, Shades of Grey, and Grey-edge performance.

Method	Parameters	Median angle	Max angle	RMS angle	Median dist ( $\times 10^2$ )	Max dist ( $\times 10^2$ )	RMS dist ( $\times 10^2$ )
Max_RGB	–	5.17	38.90	8.70	3.71	31.51	6.40
Grey World	–	6.84	47.63	9.49	5.10	41.65	7.54
SoG	$p = 6$	5.33	43.36	7.53	4.10	32.22	5.58
Grey-Edge	$e^{1,1,6}$	5.12	46.68	7.56	3.88	33.51	5.76
Second-order Grey-Edge	$e^{2,1,5}$	5.11	46.06	7.36	3.84	33.05	5.56
CCAS	$\varepsilon = 0.5, p = 6, CTimes = 5,$	5.18	43.40	7.52	3.94	32.59	5.57
CCAS (Optimized)	$Tnum = 6$	5.13	41.86	7.44	3.83	32.12	5.56

The tests are based on the more than 11,346 real-world images.

As with the distance’s measure, we also report RMS, maximum and median angular error over the test set of images.

To evaluate the error distribution difference in the performance of two competing methods, the Wilcoxon signed-rank is applied.<sup>19,27</sup> The threshold for accepting or rejecting the null hypothesis is set to be 0.01.

### 321 SFU Image Dataset

First, the proposed algorithms were tested on a large dataset of colorful objects under different light sources.<sup>25</sup> The set consists of 321 images taken under 11 varying light sources of 30 different scenes containing both matte and specular objects.

In Table I, the results of many algorithms, such as Grey World, Max-RGB, SoG, and Grey-Edge are summarized. The parameters of Grey-Edge are determined according to their best performance.<sup>7</sup> From the result shown in Tables I and II, we can find that the proposed algorithms CCAS and CCAS (optimized) outperform all other existing algorithms. Interestingly, the median angle and chromatic distance of CCAS (optimized) are 2.18 and 1.61 respectively, which reduces by 20.4 and 20.7% compared with the Second-order Grey-Edge algorithm. Table II tells us that CCAS with optimized initial value has the best performance.

### 900 Uncalibrated Image Dataset

We next consider Cardei’s set of 900 uncalibrated images taken by a variety of different digital cameras.

The experimental results are tabulated in Table III. Table IV summarizes the Wilcoxon test among several algorithms.

From Tables III and IV, the proposed algorithms CCAS and CCAS(optimized) still outperform all other algorithms. The median angle and chromatic distance of CCAS(optimized) are only 2.07 and 1.51 respectively, which reduces by 30.1 and 30.4% compared with the Max\_RGB, which is best one in existing algorithms on this dataset. Furthermore, Table IV again proves that the optimized initial value is effective and useful for CCAS.

### Large Real-World Image Dataset

Next, the color constancy algorithms were tested on a large database provided by Ciurea and Funt.<sup>26</sup> The database contains 11,346 images extracted from 2 h of digital video, which include both indoor and outdoor scenes under a wide variety of lighting conditions. Figure 4(A) gives some example images. A matte grey sphere ball was mounted onto the video camera, appearing at right-bottom corner of each image. The averaged R/G/B value on the bright part of the ball is used as the ground truth of the illumination color in the scene. As shown in Fig. 4(B), all images are cropped to remove the effect of the grey sphere ball on the algorithm. The size of the remaining image is  $240 \times 240$ . The parameters of Grey-Edge are also decided according to their best performance in.<sup>7</sup> Tables V and VI show that the performance of the proposed algorithm CCAS (opti-

TABLE VI. Comparison of CCAS to other algorithms via the Wilcoxon signed-rank test.

	Max_RGB	Grey-World	SoG	Grey-Edge	Second-order Grey-Edge	CCAS	CCAS (optimized)
Max_RGB	–	+	–	–	–	–	–
Grey World	–	–	–	–	–	–	–
SoG	+	+	–	–	–	–	–
Grey-Edge	+	+	+	–	–	+	–
Second-order Grey-Edge	+	+	+	+	–	+	=
CCAS	+	+	+	–	–	–	–
CCAS (Optimized)	+	+	+	+	=	+	–

The labelings ‘+’ ‘–’ and ‘=’ have same meanings as those shown in Table II.

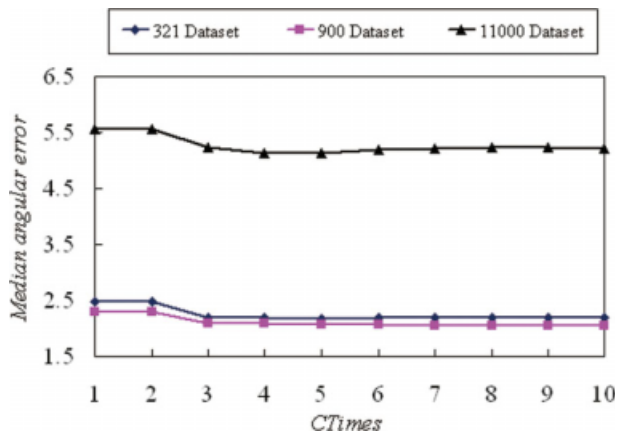


FIG. 5. The median angular errors on different datasets change with  $CTimes$ . [Color figure can be viewed in the online issue, which is available at [www.interscience.wiley.com](http://www.interscience.wiley.com).]

mized) is better than Max-RGB, Grey World, SoG, and Grey-Edge algorithms and is comparable to Second order Grey-Edge method.

### Iteration

One of the key parameters in the proposed methods is the number of iterations  $CTimes$ . In this section, we analyze its impact on the performance of CCAS (optimized). We set  $CTimes$  change from 1 to 10. The median angular errors on different datasets are used to evaluate the performance. The experimental results are shown in Fig. 5. With the  $CTimes$  increasing, the median angular errors become smaller. When  $CTimes > 5$ , the change of median angular error trends to stability. Therefore  $CTimes = 5$  would be suitable for most situations.

### Achromatic Pixels in Image Datasets

The proposed algorithms require enough achromatic pixels in the scene. Otherwise, they will reduce to the SoG algorithm. Actually, achromatic pixels often exist in mostly real environments, they are from paper, wall, clothe, floor, and others. Table VII gives out the average number of achromatic pixels detected by the proposed method CCAS (optimized) for the images in different sets. It shows that nearly 20% of image pixels are achromatic in these datasets.

TABLE VII. Average achromatic pixels detected by CCAS (optimized) in different datasets.

Dataset	Average achromatic pixels	Image size	Rate
321SFU	58352	637 × 468	19.6%
900 Uncalibrated	54212	206550 (Average)	26.2%
1,1000 Real-world	12776	240 × 240	22.2%

## CONCLUSION

In this article, we present a new color constancy method based on identifying achromatic surfaces iteratively. This method is similar to what have been proposed in GSI.<sup>8</sup> However, the achromatic surfaces detection here works on the image itself without previous knowledge of the imaging device. The local Grey Edge is also introduced to generate the optimal initial value of iteration to improve the performance of the proposed algorithm. The experiments on several real image datasets show that the method works slightly better than other typical unsupervised color constancy solutions.

## ACKNOWLEDGMENTS

The authors would like to thank Computational Vision Laboratory of Simon Fraser University for providing the image datasets.

- Barnard K, Cardei V, Funt BV. A comparison of computational color constancy algorithms-part 1: Methodology and experiments with synthesized data. *IEEE Trans Image Process* 2002;11:972–983.
- Barnard K, Martin L, Coath A, Funt BV. Comparison of computational color constancy algorithms-part 2: Experiments with image data. *IEEE Trans Image Process* 2002;11:985–996.
- van de Weijer J, Gevers Th. Color constancy based on the grey-edge hypothesis. In: *Proceeding of IEEE Conference on Image Processing*. Genoa, Italy, 2005. p 722–725.
- Finlayson GD, Drew MS, Funt BV. Color constancy: Generalized diagonal transforms suffice. *J Opt Soc Am A* 1994;11:3011–3019.
- Buchsbaum G. A spatial processor model for object colour perception. *J Franklin Inst* 1980;310:337–350.
- Finlayson GD, Trezzi E. Shades of gray and colour constancy. In: *Proceeding of 12th Color Imaging Conference*. Springfield, VA: IS&T; 2004. p 37–41.
- Weijer JV, Gevers T, Gijssenij A. Edge-based color constancy. *IEEE Trans Image Process* 2007;16:2207–2214.
- Xiong W, Funt B, Shi L. Automatic white balancing via grey surface identification. In: *Proceeding of 15th Color Imaging Conference: Color Science, Systems and Applications*. Springfield, VA: IS&T; 2007. p 5–9.
- Brainard DH, Freeman WT. Bayesian color constancy. *J Opt Soc Am A* 1997;14:1393–1411.
- Finlayson G, Hordley S, Hubel P. Color by correlation: A simple, unifying framework for color constancy. *IEEE Trans Pattern Anal Machine Intell* 2001;23:1209–1221.
- Barnard K, Martin L, Funt BV. Colour by correlation in a three-dimensional colour space. In: *Proceeding of Sixth European Conference on Computer Vision*. Dublin, Ireland, 2000. p 275–289.
- Cardei V, Funt B, Barnard K. Estimating the scene illumination chromaticity using a neural network. *J Opt Soc Am A* 2002;19:2374–2386.
- Funt B, Xiong W. Estimating Illumination Chromaticity via support vector regression. In: *Proceeding of 12th Color Imaging Conference: Color Science, Systems and Applications*. Springfield, VA: IS&T; 2004. p 47–52.
- Xiong W, Funt B. Estimating illumination chromaticity via support vector regression. *J Imaging Sci Technol* 2006;50:341–348.
- Xiong W, Shi L, Funt B. Illumination Estimation via thin-plate spline interpolation. In: *Proceedings of 15th Color Imaging Conference*. Springfield, VA: IS&T; 2007. p 25–29.
- Rosenberg C, Hebert M, Thrun S. Color constancy using KL-divergence. In: *Proceedings of IEEE International Conference on Computer Vision (ICCV)*. British Columbia, Canada, 2001. p 239–246.



17. Sapiro, Guillermo. Color and illuminant voting. *IEEE Trans Pattern Anal Machine Intell* 1999;21:1210–1215.
18. Ebner M. *Color Constancy*. England: John Wiley; 2007.
19. Xiong W. *Separating Illumination from Reflectance in Color Imagery*. Ph.D. Thesis, Simon Fraser University, British Columbia, Canada, 2007.
20. Ebner M. Combining white-patch retinex and the gray world assumption to achieve color constancy for multiple illuminants. In: *Proceedings of the 25th DAGM Symposium*. Magdeburg, Germany, 2003. p 60–67.
21. Finlayson GD, Hordley SD. Color constancy at a pixel. *J Opt Soc Am A* 2001;18:253–264.
22. Ebner M. Color constancy using local color shift. In: *Proceeding of the 8th European Conference on Computer Vision*. Prague, Czech, 2004. p 276–287.
23. Gijsenij A, Gevers T. Color constancy by local averaging. In: *Proceeding of International Conference on Image Analysis and Processing Workshops*. Modena, Italy, 2007. p 171–174.
24. Kawakami R, Ikeuchi K, Tan RT. Consistent surface color for texturing large objects in outdoor scenes. In: *Proceeding of International Conference on Computer Vision*. Beijing, China, 2005. p 1200–1207.
25. Barnard K, Martin L, Funt BV, Coath A. A data set for colour research. *Color Res Appl* 2002;27:147–151.
26. Ciurea F, Funt B. A large image database for color constancy research. In: *Proceeding of the 11th Color Imaging Conference*. Springfield, VA: IS&T; 2003. p 160–164.
27. Hordley SD, Finlayson GD. Reevaluation of color constancy algorithm performance. *J Opt Soc Am A* 2006;23:1008–1020.